

Reflection Coefficient Estimation through the Modelling of Ultrasonic Transmission

Ryuugo Mochizuki*

*Center for Socio-Robotic Synthesis, Kyushu Institute of Technology, 2-4 Hibikino Wakamatsuku
Kitakyushu, 808-0196/Fukuoka, Japan*

Yuya Nishida, Kazuo Ishii

*Department of Human Intelligence Systems, Kyushu Institute of Technology, 2-4 Hibikino Wakamatsuku
Kitakyushu, 808-0196/Fukuoka, Japan*

*E-mail: mochizuki.ryuugo126@mail.kyutech.jp, y-nishida@brain.kyutech.ac.jp, ishii@brain.kyutech.ac.jp
www.lsse.kyutech.ac.jp*

(leave space here should be 4 lines between www.university_name.edu and Abstract)

Abstract

In food industry, shortage of workers is one of a serious problem. Automation of food handling is a critical isSue nowadays. To alleviate the damage caused by food picking operation by robotic hand, we propose non-contact acoustic impedance estimation with ultrasonic wave, which should be preceded before the picking for optimization of grasp stiffness. We have the assumption of the correlation between hardness and acoustic impedance. The impedance is calculated by the product of sonic velocity and density of a medium. From the point of view, the harder the medium is, the larger the impedance should be.

We built up ultrasonic transmission model considering attenuation by ultrasonic reflection and absorption, then, made an experiment to estimate internal reflection of samples with two overwrapped media of different acoustic impedance.

Keywords: Acoustic Impedance, Ultrasonic Transmission, Hardness Estimation, Internal Reflection, Absorption

1. Introduction

In Japan, employment opportunities to both sexes have steadily increased up to now. According to the report¹, number of housewife household has been decreased by nearly two million, while, dual-income households have been increased by the same amount. Single households have been increased (for elderly, about three million, for non-elderly, about 1.5 million) for 20 years recently². As the market of prepared dishes, the magnitude has rose up by seven times from 1985 to 2016³. From the point of view, the relevance can be assumed between the demand for prepared dishes and increase of single or dual-income households. On the other hand, in food industry, the jobs-

to-applicants ratio has rose up from 1.48 to 2.78 for five years from 2013⁴, whose ratio is higher than other industry, little applicants are assumed to be willing to work for the industry. If the increase of single or dual-income households continues, the supply of prepared dishes may not be enough, thus, automation of food process and packing is one of a crucial task.

As one of the task in the automation, we aim to realize safe food picking (without damaging food) by a robot hand. To cope with the task, we propose to introduce non-contact hardness estimation with ultrasonic wave to optimize grasp stiffness, which precedes to the picking. We estimated reflection coefficient by overwrapping two

samples with different acoustic impedance, considering the value as hardness.

2. Related Work

Machado et. al. have analyzed reflected ultrasonic wave to evaluate wood strength⁵. Cho et al. have measured depth of cheeses with 99.98 % of accuracy, furthermore, succeeded in observe more than 0.9 of correlation between sonic velocity and a mechanical property of the cheese⁶. Satyam et al. estimated varying hardness of tomatoes over a time period from fresh to full ripen cycle of the crops⁷.

However, to the best of our knowledge, no report of hardness estimation considering heterogeneity of hardness has been found. The heterogeneity usually orients from uneven heating of food during cooking process, thus, we should consider the case of soft interior with hard surface.

3. Proposed Method

3.1. Outline

As the preparation, we estimate attenuation coefficient in the air α_0 and sound pressure of emitted wave P_0 , then obtain and treat emitted wave $\psi_{t,0}(t)$ in similar way as basis function for wavelet transform⁸. To analyze received wave, we consider arbitral samples as multiply overlapped media as Fig. 1 shows (z_k denotes the surface of medium k), for this reason, received wave $p_r(t)$ can be regarded as summation of reflected waves $p_{r,k}(t)$ at different surfaces of media. $p_{r,k}(t)$ is expressed in two ways, that is modelled reflection $\hat{p}_{r,k}(t)$, and reflection $\psi_{r,k}(t)$ based on $\psi_{t,0}(t)$. The former expresses relationship between reflection coefficient r_k at the surface of medium k and attenuation coefficient α_k [Np/m] inside medium k based on amplitude, however, waveform information is not considered. The latter can express waveform because $\psi_{t,0}(t)$ is stretched or compressed in two direction (time and amplitude) to fit $p_{r,k}(t)$ in this stage. The analyzation process of $p_r(t)$ is shown as Fig. 2. First, the amplitude of $p_r(t)$ is judged through the thresholding by fixed value T_p . If the judgement is true, $\psi_{t,0}(t)$ slides in the time axis' direction, then stretched or compressed in the ratio of A_k vertically and B_k horizontally so that the correlation between $\psi_{t,0}(t)$ and $p_r(t)$ is maximized, then, $\psi_{r,k}(t)$ can be

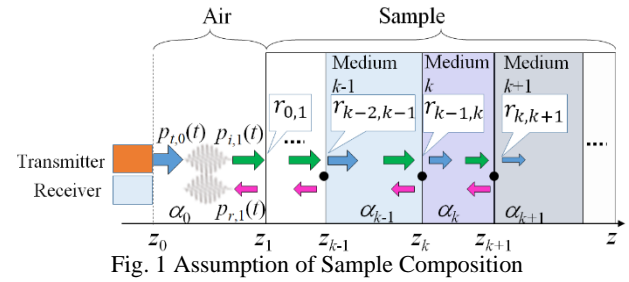


Fig. 1 Assumption of Sample Composition

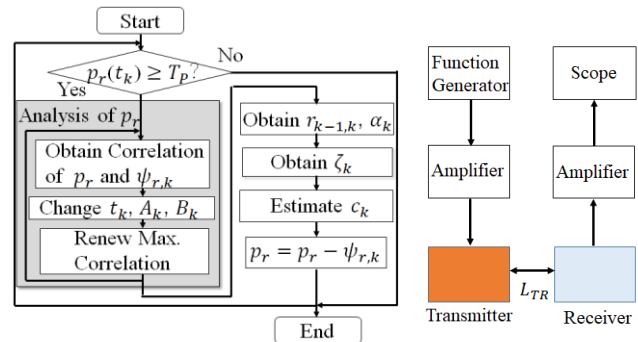


Fig. 2 Process of Analyzing p_r

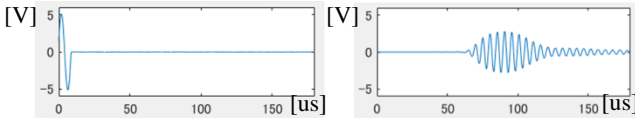
Fig. 3 Calibration Environment

obtained. We assume the amplitude of reflection is larger at closer area of sample surface, then, we limit searching area of the maximization of the correlation to $t_k > t_{k-1}$ (Here, t_k denotes estimated time of the reception of $p_{r,k}(t)$). At this stage, t_k should overwrap the maximum amplitude of $\psi_{t,0}(t)$.

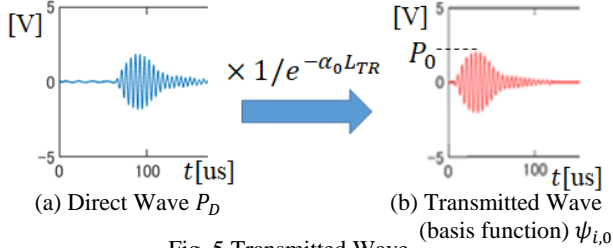
In the estimation of $\hat{p}_{r,k}(t)$, α_k and r_k are solved so that the squared error between $\hat{p}_{r,k}(t)$ and $\psi_{r,k}(t)$ is minimized. $\hat{p}_{r,k}(t)$ has another unknown parameter c_k [m/s] (sonic velocity in medium k), which is obtained through the fitting of linear function estimated from the relation between sonic velocity and acoustic impedance referring to a database. Hereafter, the estimation of α_k and $r_{k-1,k}$ proceeds with iterative subtraction by $\psi_{r,k}(t)$ from $p_r(t)$, which ends when the amplitude of p_k is less than T_p .

3.2. Calibration of attenuation coefficient and sound pressure of the emission

Sound Pressure P_0 cannot be estimated [Pa], then we assume that the pressure is proportional to output voltage [V] of the receiver. We obtain P_0 [V] and α_0 [Np/m] as the calibration process under the condition (Fig. 3) in which transmitter and receiver are aligned face to face. Function Generator generates one cycle of sign wave (Fig.4(a)) to the transmitter and direct wave is received



(a)Input of Function Generator (b)Amplified Direct Wave
Fig. 4 Transmitted Wave



(a) Direct Wave P_D (b) Transmitted Wave
(basis function) $\psi_{i,0}$
Fig. 5 Transmitted Wave

as Fig.4(b) shows. P_0 and α_0 can be calculated with the amplitudes of directed waves that are observed from a few different distances L_{TR} from the transmitter. When P_0 and α_0 are obtained, as Fig. 5 shows, cancellation of the attenuation by α_0 results in the solution of $\psi_{t,0}(t)$.

3.3. Expression of the reflected wave

$p_{r,k}(t)$ is expressed in two ways, based on transmission and attenuation model $\hat{p}_{r,k}(t)$ and $\psi_{r,k}(t)$, which is made from the compression of $\psi_{t,0}(t)$. As $\hat{p}_{r,k}(t)$, we consider the attenuation of ultrasonic wave originates from the reflection (The amplitude of the reflected wave is diminished to the ratio $r_{k-1,k}$ at location $z = z_k$) and transmission (The transmitted wave moves in velocity c_k [m/s] and the amplitude is diminished to the ratio of $e^{-c_k(z_{k+1}-z_k)}$ since its entry at $z = z_k$). After the emission of $p_{t,0}(t)$, the reflection and transmission is repeated $2k-1$, $2k$ times, each other. Thus, $\hat{p}_{r,k}(t)$ is expressed in Eq. (1), (2).

$$\widehat{p}_{r,k}(t) = r_{k-1,k} C_{\Pi,k} \psi_{i,0}(t) e^{-2\alpha_{k-1}(z_k - z_{k-1})}. \quad (1)$$

$$C_{\Pi,k} = \prod_{k'=1}^{k-1} (1 - r_{k'-1,k'}^2) e^{-2\alpha_{k'-1}(z_{k'} - z_{k'-1})}. \quad (2)$$

However, waveform is not considered in $\hat{p}_{r,k}(t)$. Even if the Function Generator generates a cycle of sine wave, the transmitted wave is shown in a scope as a group of sine waves whose amplitude changes continuously and whose frequency is equal to the central frequency f_c [Hz] of the transducer (Fig. 5). We stretch $\psi_{t,0}(t)$ A_k times vertically and B_k times horizontally as Eq. (3) shows, in this way, reflected wave based on $\psi_{t,0}(t)$ $\psi_{r,k}(t)$ can be obtained.

$$\widehat{p}_{r,k}(t) = A_k \psi_{i,0}\left(\frac{t-t_0}{B_k}\right) \quad (3)$$

We assume maximum sound pressure is measured at $t = t_0$ in case that transmitter and receiver contacts each other, and the frequency of transmitted wave changes $1/B_k$ times in media k compared to the emission.

4. Experiment

As we mentioned in Chapter 1, hardness s is considered to be acoustic impedance ζ . Here, a medium k is regarded to have a uniform ζ_k then we treat a sample as a medium. For neighboring media $k-1$ and k , ζ_k have the relationship with r_k shown in Eq. (4)¹⁰.

$$r_{k-1,k} = \frac{\zeta_k - \zeta_{k-1}}{\zeta_k + \zeta_{k-1}}. \quad (4)$$

From the point of view, large $r_{k-1,k}$ can be observed if ζ_k has large difference from ζ_{k-1} . The object of this experiment is to configure the increase of $r_{1,2}$ if ζ_2 increases. As well, ζ_2 and $r_{1,2}$ should have the same relation even if the depth of samples H_S (H_{S1} , H_{S2} for Sample 1, 2 each other) changes. Table 1 shows the pattern of sample combination, here we selected $H_{S1} = 29$ [mm] for pattern 1, 2, and $H_{S2} = 35$ [mm] for pattern 3, 4. We only consider positive reflection coefficient.

4.1. Preparation

We recorded amplitude P_D of direct wave using the environment shown in Fig. 3 and changing $L_{TR} = 10, 20, \dots, 50$ [mm]. We expect that P_D attenuates under extended L_{TR} following Eq. (5), with reference of $L_{TR} = L_{TR,1} (= 20$ [mm]), then iteratively estimated α_0 and P_0 for 20 times.

$$P_D(L_{TR}) = P_D(L_{TR,1}) e^{-\alpha_0(L_{TR} - L_{TR,1})}. \quad (5)$$

$$P_0 = P_D(L_{TR,1}) e^{\alpha_0 L_{TR,1}}. \quad (6)$$

4.2. Environment

Fig. 6 shows the environment for reflection estimation, and, Fig. 7 shows used samples. The true value of ζ and c is summarized in Table 1. ζ can be expressed in another way in Eq. (7), with the relationship between ζ and c , here, ρ [kg/m³] denotes sample density⁹.

Table 1 True Value of Sonic Speed c and Acoustic Impedance ζ (at Temperature 30[deg])

Sample Name	H_S [mm]	c [m/s]	ζ [Pa s/m]
Al	10	6420	17.3×10^6
Gel (s=0)	29	2237	2.5×10^6
	35	2233	2.4×10^6
Gel (s=7)	30	2185	2.5×10^6
	36	1643	1.8×10^6

Table 2 Setting for the Experiment

T_P	$P_0/100$	f_c	200[kHz]
H_E	50[mm]	τ	$\pm 40V$ (Calib.)21[deg]
θ_1	15[deg]		(Ref.)21[deg]
P_0	$\pm 40V$		$\pm 50V$ (Calib.)21[deg]
	$\pm 50V$		(Ref.)24[deg]
α_0	$\pm 40V$	a_1	$471.1[m/(Pa s^2/m)]$
	$\pm 50V$		a_2

Table 3 Combination of Samples

Pattern	Sample 1		Sample 2	
	Sample Name	H_{S1} [mm]	Sample Name	H_{S2} [mm]
1	Gel (s=0)	29	Gel (s=7)	30
2	Gel (s=0)	29	Al	10
3	Gel (s=0)	35	Gel (s=7)	36
4	Gel (s=0)	35	Al	10

$$\zeta = \rho c. \quad (7)$$

Urethane Gel is produced through the mixture and coagulation of two kinds of liquid. thus, H_S is not uniform. We measured H_S in the environment shown in Fig. 8, by sandwiching the sample by a transmitter and receiver, then subtracting L_2 from L_1 , and, obtained true c by measuring elapsed time from wave emission to reception and dividing H_S with the time. As the true ζ , we used Eq. (7) to obtain. However, as ζ of aluminum, we referred to Ref. 11 because the media has extremely large ζ . As the calibration to decide α_0 and P_0 , we repeated for 20 times, and averaged the results of the estimations. Table 2 shows the setting of experiment(central frequency f_c , distance from transmitter and sample surface H_E , stilt of transducers θ_1 , temperature τ), and estimation of α , P_0 . The amplitude of the input to transmitter was $\pm 40, \pm 50[V]$. The coefficient a_1, a_2 of the linear function to find sonic

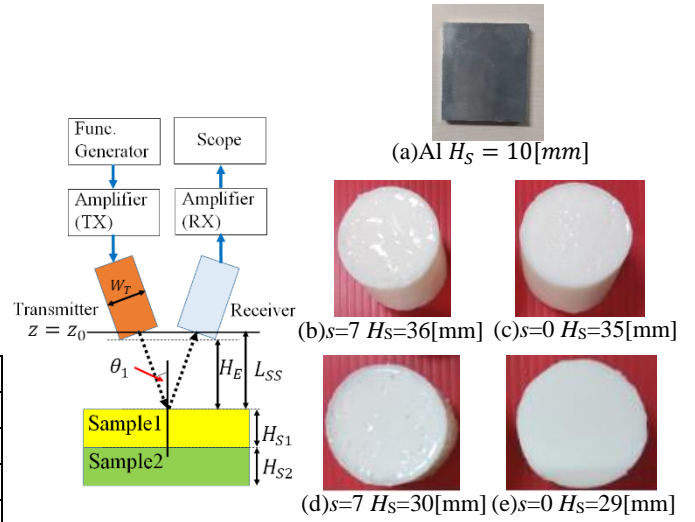


Fig. 6 Experimental Environment

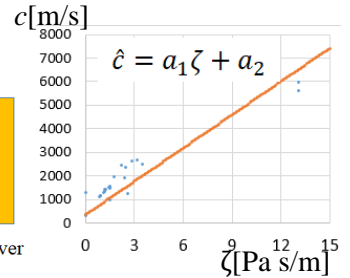


Fig. 9 Estimation of c with input of ζ

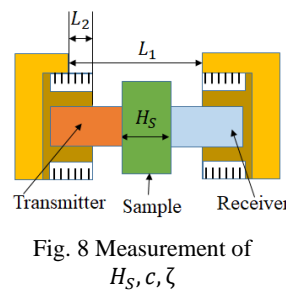


Fig. 8 Measurement of H_S, c, ζ

velocity is shown in the table as well. a_1 differs from ρ in that a_1 is regarded uniform, while ρ synchronously changes as c changes. Table 3 shows the patterns of the sample combination, that is, material name, s, H_S .

4.3. Result and Discussion

Table 4 shows the estimation result (average and standard deviation of $r_{0,1}, r_{1,2}$) totally. As under condition $\pm 40[V]$ is input to transmitter, Fig. 10, Fig. 11 shows the comparison of $r_{1,2}$, the former is of pattern 1 and 2, the latter is of pattern 3 and 4. As under condition

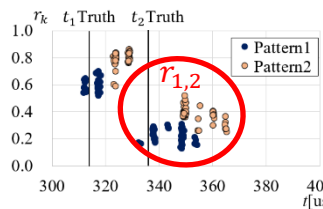


Fig. 10 Result of $r_{k-1,k}$ Estimation for Pattern 1, 2 (Input: $\pm 40[V]$)

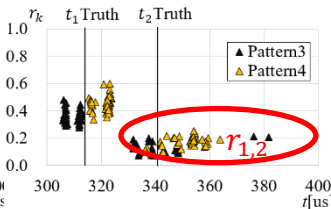


Fig. 11 Result of $r_{k-1,k}$ Estimation for Pattern 3, 4 (Input: $\pm 40[V]$)

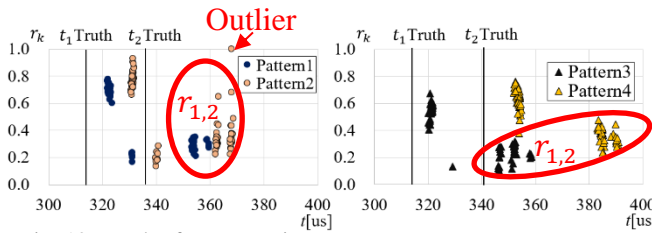


Fig. 12 Result of $r_{k-1,k}$ Estimation for Pattern 1, 2 (Input: $\pm 50[V]$)

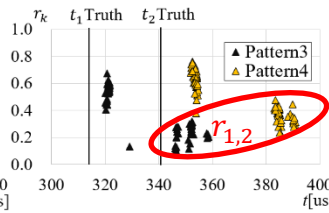


Fig. 13 Result of $r_{k-1,k}$ Estimation for Pattern 3, 4 (Input: $\pm 50[V]$)

Table4 Summary of Reflection Coefficient Estimation Result

		Input $\pm 40[V]$	Input $\pm 50[V]$
Average of $r_{0,1}$	Pattern1	0.60	0.71
	Pattern2	0.79	0.76
	Pattern3	0.36	0.56
	Pattern4	0.45	0.64
Standard Deviation of $r_{0,1}$	Pattern1	0.05	0.04
	Pattern2	0.05	0.05
	Pattern3	0.05	0.06
	Pattern4	0.05	0.08
Average of $r_{1,2}$	Pattern1	0.22	0.29
	Pattern2	0.37	0.32
	Pattern3	0.15	0.24
	Pattern4	0.18	0.36
Standard Deviation of $r_{1,2}$	Pattern1	0.05	0.04
	Pattern2	0.06	0.10
	Pattern3	0.08	0.06
	Pattern4	0.03	0.05

$\pm 50[V]$ is input to transmitter, Fig. 12, Fig. 13 shows the comparison of $r_{1,2}$, the former is of pattern 1 and 2, the latter is of pattern 3 and 4. where $r_{1,2}$ is surrounded by an oval. As Table 4 shows, pattern 2 shows higher $r_{1,2}$ than pattern 1 and, pattern 4 shows higher $r_{1,2}$ than pattern 3, where the result (increase of ζ_2 resulted in rising $r_{1,2}$.) could be found. However, the 40[us] of delay in t_1 was shown in pattern4 of Fig. 13, which was mainly caused by heterogeneity of sample depth. To reduce the error, bump or inclination of sample surface should be eliminated under coagulation.

4.4. Conclusion

As the result of the experiment, we succeeded in observing larger $r_{1,2}$ according to the increase of ζ_2 , which may show the possibility of estimating the variety of hardness inside samples.

References

1. “The Japan Institute for Labour Policy and Training,” <https://www.jil.go.jp/kokunai/statistics/timeseries/html/g0212.html> (in Japanese)
2. “Yahoo News,” <https://news.yahoo.co.jp/byline/fuwarazo/20130909-00027589> (in Japanese)
3. “Ministry of Agriculture, Forestry and Fisheries HP,” https://www.maff.go.jp/j/wpaper/w_maff/h29/h29_h/trend/part1/chap2/c2_6_00.html
4. “Ministry of Agriculture, Forestry and Fisheries HP,” <https://www.maff.go.jp/j/press/shokusan/seizo/attach/pdf/190711-2.pdf>
5. J Machado, P. Palma, S. Simoes, “Ultrasonic Indirect Method for Evaluating Clear Wood Strength and Stiffness”, Non-Destructive Testing in Civil Engineering, pp. 1-6, 2009,
6. B. Cho and J. Irudayaraj, “A Noncontact Ultrasound Approach for Mechanical Property Determination of Cheeses”, Food Engineering and Properties, Vol.68, No. 7, pp. 2243-2247, 2003.
7. S. Srivastava, S. Vaddadi and S. Sadistap, “Non-Contact Ultrasonic Based Stiffness Evaluation System for Tomatoes during Shelf-Life Storage”, Journal of Nutrition and Food Sciences, Vol. 4, Issue 3, pp 1-6, 2014.
8. R.K.Young,N.K.Bose,“Wavelet Theory and Its Applications”,Kluwer Academic Publishers,1993.
9. J. Carlson, J. Deventer, A. Scolan and C. Carlander, “Frequency and Temperature Dependence of Acoustic Properties of Polymers Used in Pulse-Echo Systems”, Proceedings in IEEE Symposium on Ultrasonics, pp. 885-888, 2003.
10. S. Takeuchi, Tutorial on the underwater or medical ultrasound transducer, (In Japanese) J. Acoust. Soc. of Japan, Vol. 72, No. 5, pp. 264-272, 2016.
11. Honda Electronics Co., Ltd. “Ultrasound Handbook,” (In Japanese), 2008.

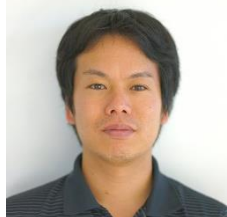
Authors Introduction

Dr. Ryuugo Mochizuki



He is a researcher at Graduate School of Life Science and System Engineering, Kyushu Institute of Technology, Japan. His research topic during the PhD course was image processing. Currently, he is involved in signal processing of ultrasonic.

Dr. Yuya Nishida



He is an Associate Professor at Graduate School of Life Science and System Engineering, Kyushu Institute of Technology, Japan. His research area is about field robotics, its application, and data processing.

Prof. Kazuo Ishii



He is a Professor at Graduate School of Life Science and System Engineering, Kyushu Institute of Technology, Japan. His research area is about field robots and intelligent robot system